JPEDAV (2005) 26:417-422
DOI: 10.1361/154770305X66457
1547-7037/$19.00 ©ASM International

Modeling Silicon and Aluminum Diffusion in Electrical Steel

Jose Barros, Benny Malengier, Roger Van Keer, and Yvan Houbaert

(Submitted July 12, 2005)

High silicon (Si) and aluminum (Al) electrical steel with improved magnetic properties can be produced by hot dipping in a molten Al-25 wt.% Si bath followed by diffusion annealing. The hot dipping deposits a Si-rich layer on top of the substrate, which is subsequently diffused into the bulk at high temperatures. The final properties of the material depend on the resulting concentration profiles, therefore a model capable of simulating the Si and Al diffusion is required. The first steps toward such a model are presented. The lack of knowledge of the ternary interdiffusion coefficients for the Al-Si-Fe system is overcome by reducing the coupled system of diffusion equations to a single partial differential equation (PDE), utilizing the diffusion path. Then by using a Levenberg-Marquardt inverse method, the apparent diffusion along this path can be determined. The direct problem was solved by a second-order space discretization, reducing the diffusion equation to a nonlinear system of ordinary differential equations (ODEs), which consequently can be solved with standard procedures for ODE.

1. Introduction

Electrical steel is an excellent soft magnetic material used for the construction of electrical motors and transformers. Its composition is basically high-purity Fe-Si or Fe-Si-Al alloys; normally the alloying content never exceeds 3 wt.%. Beyond this concentration the material becomes very brittle because of the concurrence of the ordering phenomena $D0_3$ and $B2$, and it is not possible to perform cold rolling.[1]

However, the magnetic properties, namely power losses and magnetostriction, are optimized when the alloying content reaches 6.5 wt.%. These higher-silicon content alloys can only be manufactured if an additional final step is introduced in the production route of electrical steel: enrichment by surface deposition of Si and Al and their diffusion into the bulk material. Recent research has shown that the magnetic and mechanical properties of the high-Si electrical steel produced by diffusion depend strongly on the shape of the diffusion profile obtained after the annealing.[2] The different applications of the electrical steel require different magnetic and mechanical properties, hence a diffusion model capable of predicting the diffusion profiles depending on the different conditions of the production process (e.g., annealing temperature, time, Si and Al content of the substrates, microstructure before the diffusion annealing) is necessary.

The aim of this study is to show the first steps toward such a model.

2. Experimental Procedures

The substrates chosen for the production of the high-Si and Al alloys were commercial Fe-Si alloys (0-3 wt.% Si). After degreasing, the electrical steel plates were subjected to the hot dipping. First the samples were preheated for 45 s at 800 °C, and then dipped in a molten Al-25 wt.% Si bath at 800 °C for times ranging between 5 and 100 s. Finally the samples cooled down under a flux of N_2. After hot dipping the specimens were heated in a resistance tube furnace under a N_2 protective atmosphere. The temperatures ranged between 900 and 1100 °C. Samples were carefully polished, and the concentration profiles through the thickness of the samples were determined by energy dispersive spectroscopy (EDS) in the scanning electron microscope (SEM). EDS was also used to analyze element concentration in the different layers of the coating.

3. Results

3.1 Coating Composition and Formation

The coating formation is a reaction-diffusion process. Together with intermetallic growth there is substrate dissolution in the molten bath. Both processes are dependent on the chemical composition of the substrate and on the dipping parameters, such as sample temperature prior to dipping, dipping time, and cooling rate after dipping as discussed in Ref 3.

Figures 1 and 2 show the appearance of the coating after the hot dipping and fast cooling (450 °C/min) and slow cooling (30 °C/min), respectively. The chemical composition of the different intermetallic layers can be found in Table 1. In the fast-cooled samples the first layer in contact

This article is a revised version of the paper printed in the *Proceedings of the First International Conference on Diffusion in Solids and Liquids - DSL-2005*, Aveiro, Portugal, July 6-8, 2005, Andreas Öchsner, José Grácio and Frédéric Barlat, eds., University of Aveiro, 2005.

Jose Barros and **Yvan Houbaert,** Department of Metallurgy and Materials Science, Gent University, Technologiepark 903, B-9052 Zwijnaarde-Gent, Belgium; and **Benny Malengier** and **Roger Van Keer,** Department of Mathematical Analysis, Gent University, Galglaan, 9000 Gent, Belgium. Contact e-mail: jose.barroslorenzo@ugent.be.

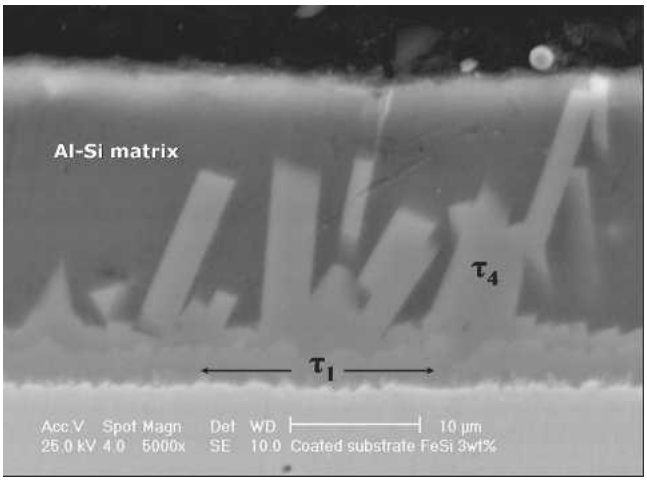

Fig. 1 Coating for Fe-Si 3 wt.% fast cooled

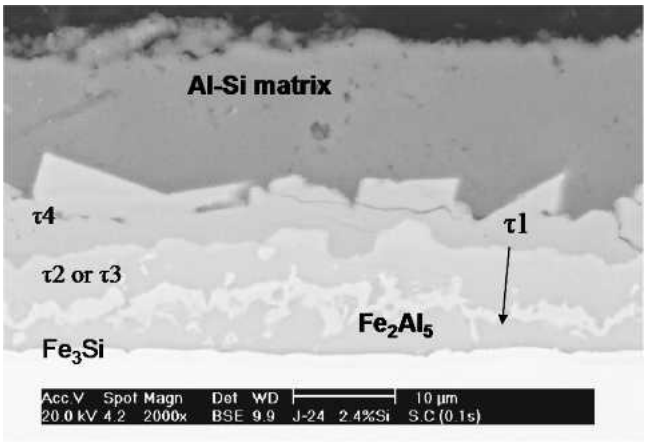

Fig. 2 Coating for Fe-Si 2.4 wt.% slow cooled

with the substrate is τ_1. A very irregular τ_4 layer grows over the τ_1. Finally, the external layer is an eutectic Al-Si matrix in which there can be found pure Si areas. Additional layers such as Fe_3Si, Fe_2Al_5, and τ_2-τ_3 appear in the slow-cooled samples.

The samples were dipped for 5 s to avoid mass loss by dissolution in the molten bath.

The chemical composition through the coating thickness can be found in Fig. 3. The diffusion path followed during the coating formation at 800 °C is depicted in Fig. 4.[4]

3.2 Diffusion Annealing[5,6]

The main diffusion annealing parameters are time and temperature, and they will determine not only the final concentration profiles of Si and Al but also the resulting texture of the material and therefore its mechanical and magnetic properties. For the diffusion experiments, substrates containing 3wt.%Si were chosen to ensure ferritic phase in the entire range of temperatures. The annealings were performed at 1100 °C. At this annealing temperature the ternary diagram simplifies, and, as shown in Fig. 5, diffusion takes place mainly in the α-phase. A typical diffusion profile can be seen in Fig. 6.

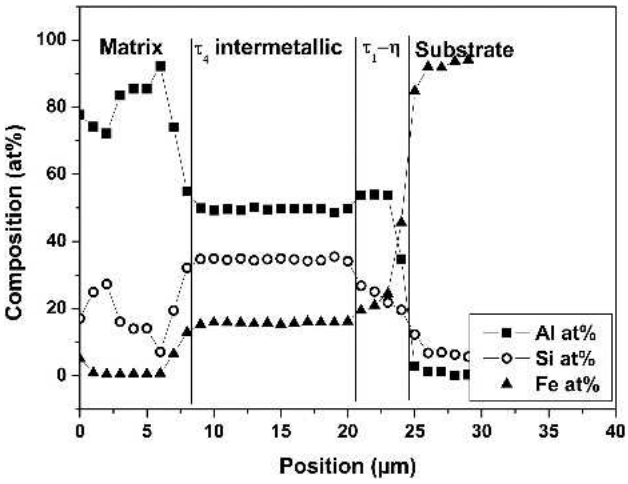

Fig. 3 Composition through the thickness for the coating for Fe-Si 3 wt.%

Table 1 Theoretical and measured composition of the intermetallic compounds

		Theoretical at.%			Measured at.%		
Phase	Composition	Al	Fe	Si	Al	Fe	Si
τ_1	$Al_{0.42}Fe_{0.39}Si_{0.19}$	42	39	19	39.20	34.30	26.50
τ_9	$Al_{0.36}Fe_{0.36}Si_{0.28}$	36	36	28	39.20	34.30	26.50
τ_2	$Al_{0.54}Fe_{0.26}Si_{0.20}$	54	26	20	52.30	24.40	23.30
τ_3	$Al_{0.50}Fe_{0.25}Si_{0.25}$	50	25	25	52.30	24.40	23.30
τ_4	$Al_{0.48}Fe_{0.15}Si_{0.37}$	48	15	37	50.20	16.60	33.16
η	Fe_2Al_5	71	29	…	69.4	30.6	…
$D0_3$	Fe_3Si	…	75	25	…	77.50	22.50

4. Mathematical Model of Diffusion Annealing

As is clear from the work of Rabkin et al.,[7] the Fe-Si interdiffusion is highly dependent on the Si concentration. Therefore, taking into account the dependence of the diffusion D on the Si concentration, C, is indispensable. This ternary system is analogous to Ref 6. The diffusion equation to be used is therefore, with $i = 1$ (Si), 2 (Al):

$$\frac{\partial C_i^3(x,t)}{\partial t} = \frac{\partial}{\partial x}\left(D_{i1}^3(C_1^3, C_2^3)\frac{\partial C_1^3(x,t)}{\partial x} + D_{i2}^3(C_1^3,C_2^3)\frac{\partial C_2^3(x,t)}{\partial x}\right) \quad \text{(Eq 1)}$$

where $0 \le x \le L$, $0 \le t < \infty$, and the superscript 3 indicates the dependent element (Fe). Furthermore, there are the no-flow boundary conditions:

$$\frac{\partial C_i^3(0,t)}{\partial x} = 0 = \frac{\partial C_i^3(L,t)}{\partial x} \quad \text{(Eq 2)}$$

and initial conditions:

$$C_i^3(x,0) = C_{0,i}^3(x) \quad \text{(Eq 3)}$$

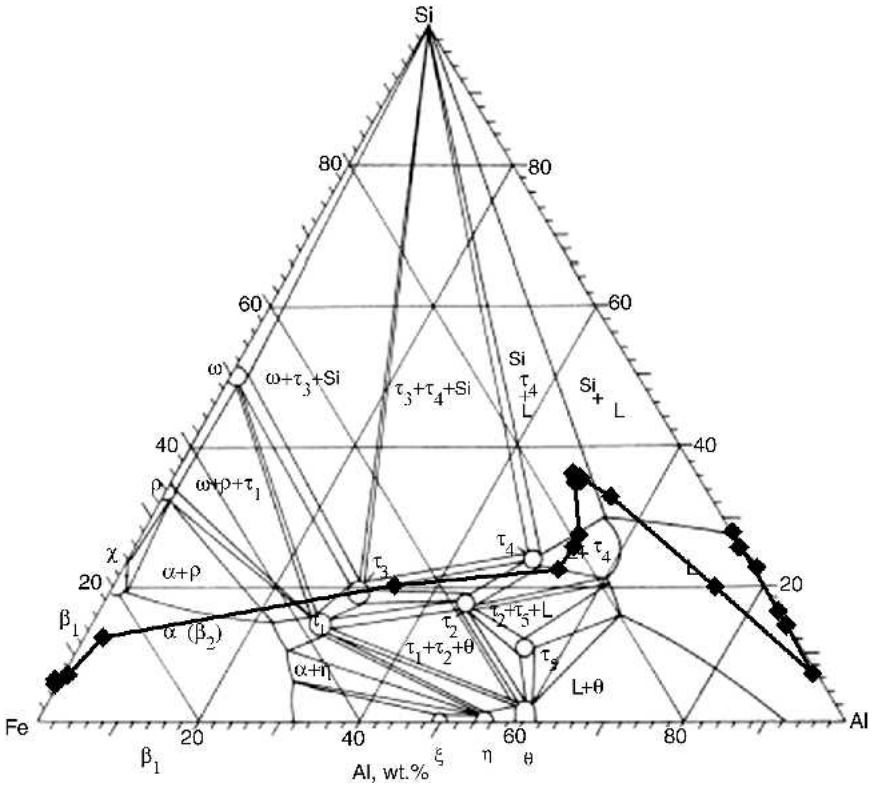

Fig. 4 Ternary phase diagram for Fe-Si-Al at 800 °C[4] and diffusion path at 800 °C for 5 s dipping, fast-cooled Fe-Si 3 wt.% substrate

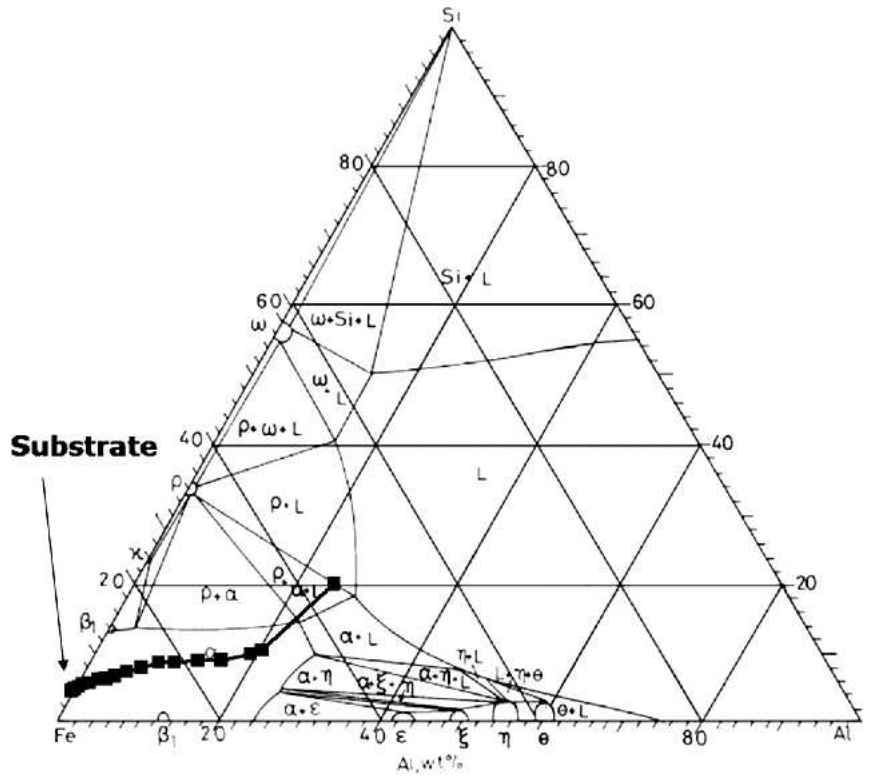

Fig. 5 Ternary phase diagram for Fe-Si-Al at 1100 °C[4] and diffusion path at 1100 °C for 5 min, Fe-Si 3 wt.%

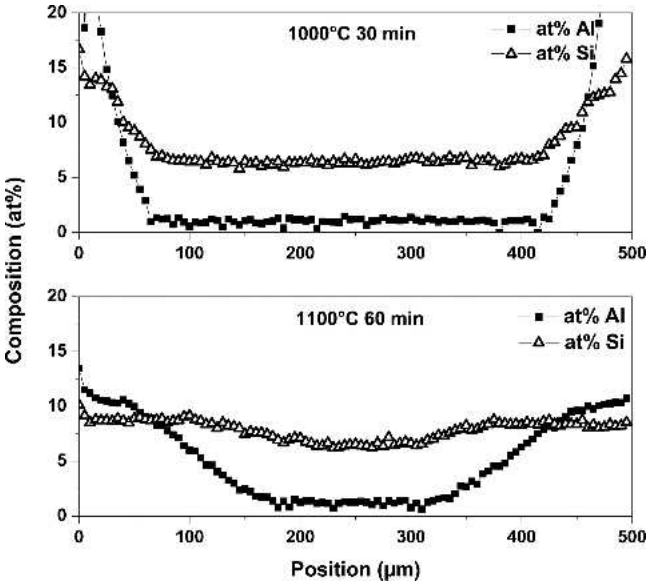

Fig. 6 Diffusion profiles for samples annealed at 1000 °C for 30 min (top) and at 1100 °C for 60 min (bottom)

The silicon concentration C_1^3, (mol/mm^3) is obtained from:

$$C_1^3 = \frac{x_{Si}}{x_{Si}v_{Si} + x_{Al}v_{Al} + (100 - x_{Si} - x_{Al})v_{Fe}} \quad \text{(Eq 4)}$$

where x_i is the atomic percent and v_i is the molar volume of each element ($v_{Si} = 12.0 \times 10^3$, $v_{Al} = 10.0 \times 10^3$, $v_{Fe} = 7.10 \times 10^3$ mm^3/mol). The Al concentration is obtained in the same way.

The work is done in one dimension, so Eq 1 to 3 can only be used once the coating has been made homogeneous in the lateral direction. Therefore, as an initial condition for this system the measured concentration profile was used after some minutes of diffusion annealing.

The main problem in solving Eq 1 to 3 is the fact that the interdiffusion coefficients D_{ij}^3 are unknown. Therefore, not only must the equations be solved, but at the same time it is necessary to extract from the experiments these interdiffusion coefficients.

The first step is to simplify the coupled system of partial differential equations (PDEs), to a single PDE. For this the authors used the fact that the diffusion path during diffusion annealing is monotone in the Al-Si concentration (Fig. 5). This implies that the authors can assume that the diffusion path is a well-defined function that can be written:

$$C_2^3 = f(C_1^3) \quad \text{(Eq 5)}$$

so given the atomic percent of Si in our steel, the value of Al can be extracted along the diffusion path.

Under the above assumption, the PDE system decouples and can be written formally:

$$\frac{\partial C_1^3(x,t)}{\partial t} = \frac{\partial}{\partial x}\left(D_1^{23}[C_1^3(x,t)] \frac{\partial C_1^3(x,t)}{\partial x} \right) \quad \text{(Eq 6)}$$

where $0 \le x \le L$, $0 \le t < \infty$, and D_1^{23} is the apparent diffusion coefficient of Si in Fe along the diffusion path f. Again, there are the noflow boundary conditions:

$$\frac{\partial C_1^3(0,t)}{\partial t} = 0 = \frac{\partial C_1^3(L,t)}{\partial x} \quad \text{(Eq 7)}$$

and initial condition:

$$C_1^3(x,0) = C_{0,1}^3(x) \quad \text{(Eq 8)}$$

As will be shown, this approach allows the extraction of the value of $D_1^{23}(C_1^3)$ from the experiments. First, section 5 will show the numerical approximation used to solve Eq 6 to 8.

5. Numerical Approximation

For simplicity, the authors will only consider the case of steels with Si 3 wt.%. Therefore there are no phase changes, and the authors assume $D_1^{23}(C_1^3) > 0$ in the entire domain.

Given the apparent diffusion coefficient $D(C_1^3) \approx D_1^{23}(C_1^3)$, system Eq 6 to 8 can be solved as in Ref 5. Here the authors suggest a different approach.

Construct the solution $C_1^3(x,t)$ of Eq 6 to 8 in an approximative way by reducing it to an initial value problem for a nonlinear system of ordinary differential equations (ODEs) by means of a nonequidistant finite difference discretization with respect to the space variable. Next, a stiff ODE solver is used to solve the system of ODEs.

The interval $(0,L)$ is partitioned by the set of grid points $\{x_i\}_{i=0}^N$. We denote $C_i(t) \approx C_1^3(x_i,t)$ and let $l_2(x, i)$ stand for the Lagrange polynomial of the second order interpolating the points (x_{i-1}, C_{i-1}), (x_i, C_i) and (x_{i+1}, C_{i+1}). Then, approximate $\partial_x C$ by $dl_2(x_i,i)/dx \equiv (dl_2(x,i)/dx)_{x=xi}$ and $\partial_x^2 C$ by $d^2l_2(x_i,i)/dx^2 \equiv (d^2l_2(x_i)/dx^2)_{x=xi}$. Because of the Neumann BCs, extend the governing PDE to the boundary points and discretize it in a way similar to that for the inner points by introducing the fictive points y_{-1}, y_{N+1}, which have their concentration values so as to satisfy the BCs. Equation 6 leads to the system of ODEs:

$$\frac{d}{dt}C_i(t) - D(C_i)\frac{d^2}{dx}l_2(x_i,i) - D'(C_i)\left[\frac{d}{dx}l_2(x_i,i)\right]^2 = 0 \quad \text{(Eq 9)}$$

for $i = 0, \ldots, N$, where

$$D' = \frac{dD(s)}{ds} \quad \text{(Eq 10)}$$

This system of nonlinear ODEs can then be solved using a standard package for stiff ODE, e.g., LSODA.

Having a solver for the direct problem Eq 6 to 8, the inverse problem of determining $D_1^{23}(C_1^3)$ is solved with a standard Levenberg-Marquardt method. For this, the au-

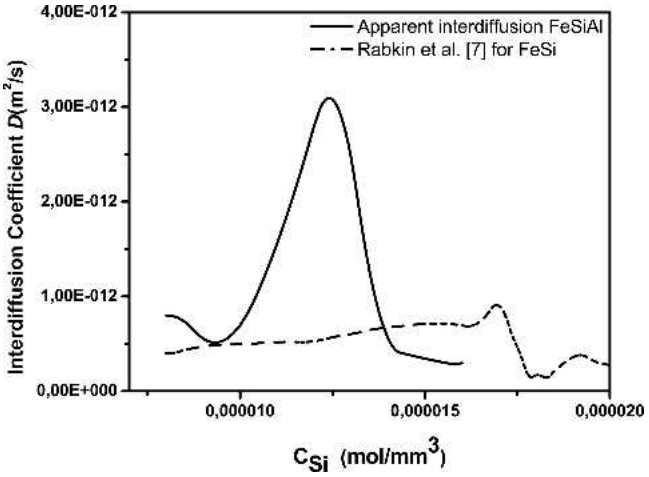

Fig. 7 Apparent diffusion coefficient at 1100 °C for the Fe-Si-Al ternary alloy (solid lines) and Fe-Si interdiffusion coefficient (dashed lines), in m^2/s

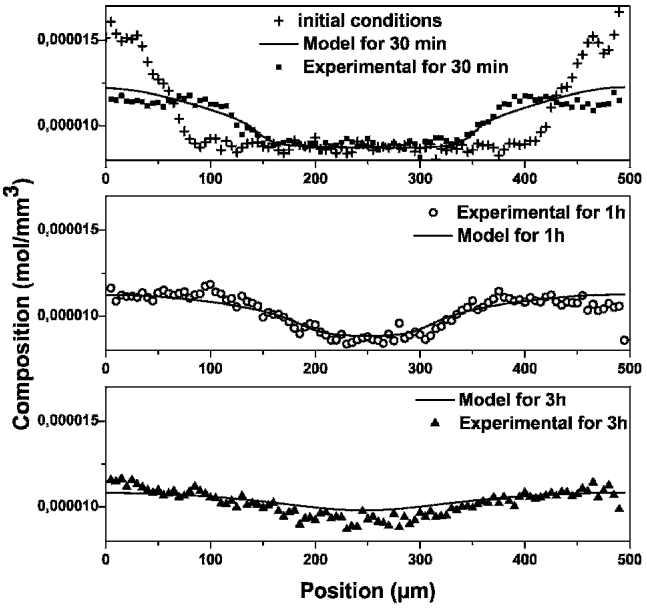

Fig. 8 Experimental and modeled concentration profiles for 5 min, 30 min, 1 h, and 3 h at 1100 °C

thors modeled the apparent diffusion by a second-order natural bspline interpolation b of couples (C_k, p_k), $k = 1, \ldots, M$,

$$D_1^{23}(C_1^3) \approx b(C_k, p_k) \qquad k = 1, \ldots, M \qquad \text{(Eq 11)}$$

Here, the points C_k can only be chosen in the relevant domain where there is experimental data, and p_k are the parameters that will be optimized with the inverse procedure. So an iteration scheme is started, beginning from the initial parameter set $\{p_k^0\}$, to determine an optimal parameter set $\{\tilde{p}_k\}$, which approximates the experimental curves as close as possible. See, e.g., Ref 8 for a possible implementation.

Summarized, the computation procedure is as follows:

1. Set the grid $\{x_i\}$; in the case of an equidistant grid the grid size Δx suffices.
2. Load the initial condition $C_{0,1}$.
3. Load the initial apparent diffusion $D(C_1^3)$ as a set of M couples (C_k, p_k^0).
4. Construct the system of nonlinear ODEs (Eq 9) where $D(C)$ is the bspline interpolation of the M couples (C_k, p_k^j).
5. Solve the system of ODEs, e.g., using LSODA.
6. Determine with the Levenberg-Marquardt method a new set of parameters $\{p_k^{j+1}\}$.
7. Go to 4 as long as the approximation improves.

6. Results of the Model

In the following numerical experiments 41 grid points x_i over the interval (0 µm, 500 µm) were used. The diffusion coefficient was constructed with eight couples (C_k, p_k), where $C_1 = 0.8e\text{-}5$ and $C_8 = 1.7e\text{-}5$. As initial values for the parameters p_k the values were taken from Ref 7, which is the Si-Fe interdiffusion (0 at.%Al). These values are shown in Fig. 7. As an initial condition for the concentration, the experimental data of 5 min of diffusion annealing was used.

Running the Levenberg-Marquardt method to find the optimal values of p_k, the authors obtained the interdiffusion coefficient as depicted in Fig. 7. The result of the direct model with this optimal D is given in Fig. 8. for the three time steps where we have experimental data. The modeled curves are good approximations of the experiments except for the 3 h curves. However, for the longest annealing times the authors detected mass loss specifically of aluminum. This phenomenon is not included in the model, and it probably explains the deviation. More experimentation will be needed to quantify this mass loss.

7. Conclusions

The authors have shown how diffusion annealing can be modeled by a single differential equation and how the lack of knowledge of the interdiffusion coefficients can be overcome. The solution was in good agreement with the experimental results; however, no exact match was obtained. Further validation of the method will be needed; the model must be refined to allow more grid points and especially more parameters to approximate the apparent diffusion. These are now limited by the computing time, however this is probably because a symbolical software was used to do the computations.

However, using a diffusion path, instead of a smeared-out diffusion zone, can also be the reason for the deviation found. A full model, solving Eq 1 to 3 should be considered. It is unclear however if the fact that the interdiffusion coefficients are unknown can be overcome in this more complicated setting.

References

1. D. Ruiz, T. Ros, R.E. Vandenberghe, and Y. Houbaert, On the Influence of Order on the Soft Magnetic Properties of Fe-Si Alloys, *Steel Res.,* Vol 76 (No. 6), 2005, p 429-435
2. J. Barros, T. Ros, L. Vandenbossche, L. Dupré, J. Melkebeek, and Y. Houbaert, The Effect of Si and Al Concentration Gradients on the Magnetic Properties of Electrical Steel, *J. Magnetism Magnet. Mater.,* Vol 290-291, 2005, p 1457-1460
3. J. Barros, T. Ros, and Y. Houbaert, Chemical and Physical Interaction of Si-Rich Steel Substrates with a Molten Al-25% Si Bath, *Defect Diffus. Forum,* Vol 237-240, 2005, p 1115-1120
4. T. Maitra and S.P. Gupta, Intermetallic Compound Formation in Fe-Si-Al Ternary System, *Mater. Char.,* Vol 49 (No. 9), 2002, p 269-311
5. K. Murakami, N. Nishida, K. Osamura, Y. Tomota, and T. Suzuki, Aluminization of High-Purity Iron by Powder Liquid Coating, *Acta Mater.,* Vol 52, 2004, p 1271-1281
6. K. Murakami, N. Nishida, K. Osamura, Y. Tomota, and T. Suzuki, Aluminization of High-Purity Iron and Stainless Steel by Powder Liquid Coating, *Acta Mater.,* Vol 52, 2004, p 2173-2184
7. E. Rabkin, B. Straumal, E. Semenov, W. Gust, and B. Predel, The Influence of an Ordering Transition on the Interdiffusion in Fe-Si Alloys, *Acta Metall. Mater.,* Vol. 43 (No. 8), 1995, p 3075-3083
8. W.H. Press, S.A. Teukolsky, W.T. Vetterling, and B.P. Flannery, *Numerical Recipes in C++: The Art of Scientific Computing,* 2nd ed., Cambridge University Press, Cambridge, 2002